Noise Modeling Methodology for Full-System Inertial Microsensor Codesign

M.D. Pottenger and W.J. Kaiser

University of California, Los Angeles
Department of Electrical Engineering
420 Westwood Plaza, Los Angeles, CA 90095-1594

ABSTRACT

Methods for incorporating noise models into full-system inertial microsensor simulation are presented. Thermal motion of the proof mass and flicker noise in the interface circuit exhibit essential behavior that must be included in sensor design. While typically described in terms of frequency spectra, these noise sources must be developed for transient simulation—inertial microsensors display nonlinearity and time dependence that invalidates any small-signal frequency domain simulation. The methods for thermal noise modeling also allow transfer function data to be obtained. Results are given for flicker noise characterization and a voltage-controlled oscillator, including both magnitude and phase information. The noise modeling methods complement a complete inertial microsensor simulation model that has been developed in the SPICE circuit simulator environment.

Keywords: inertial sensor, noise, simulation, SPICE

1 INTRODUCTION

Micromachined inertial sensors are truly integrated electromechanical devices. A mechanical input such as acceleration or rotation is converted by the sensor mass to a voltage or current. Yet currently available CAD tools can only model portions of such a system: FEA tools for the coupled electromechanical forces exerted on the mass, and more traditional applications of CAD tools for circuit design. Whereas the mechanical and electrical design of traditional inertial sensors could be performed separately, such an approach violates the very nature of solid-state microsensors. Furthermore, as the degree of CAD tool specialization increases, so do the barriers of integration as mechanical, electrical and fabrication process designers share increasingly less and less of a common design environment language. Yet the nature of such sensors demands an integrated design solution.

Codesign is a strategy for the design, synthesis and integration of complex systems composed of disparate pieces. The codesign emphasis here targets a single integrated tool capable of modeling both electromechanics of the proof mass and state-of-the-art interface and control circuits, thus eliminating the need for the sensor designer to bridge the shortcomings of existing tools. CAD tools capable of system-level integration are required for the next generation of inertial microsensor products.

There are a host of examples of codesign principles in inertial microsensor design. These are inherently coupled electromechanical systems, with both mechanical and electrical signal and noise sources. The role of noise in inertial microsensor design cannot be overstated, particularly with the growing awareness for the need for closed-loop sensor systems. While the design of many modern systems must address noise requirements of one form or another, *inertial microsensors are noise-limited systems*. Thus, while the design of a high-speed operational amplifier for a signal processing application must necessarily consider the noise floor of the opamp, this noise value may not ultimately define a fundamental limit of the signal processing. Sense amps in memory circuits are an even better example, if only because while they operate in an extremely noisy environment their own noise floors are not prime design considerations (which are typically area, power dissipation and speed).

To illustrate the importance of noise in inertial microsensor design—and to contrast this last example of memory read/write circuits—consider the sensors used for seismometry: very high performance acceleration sensors whose noise performance with respect to earth vibration is often characterized by not just their ability to detect the effects of ocean waves on the earth's shell, but how remote these waves are from the sensor location. Noise performance ultimately decides inertial microsensor performance, and the coupling of the electromechanical signal and noise sources places a profound premium on the designer to not only understand but be able to incorporate such essential behavior in the design cycle.

2 INERTIAL SENSOR MODEL

As shown in Figure 1, a complete sensor simulation model consists of a proof mass, capacitor bridge, measurement and control circuits, plus any appropriate signal and noise sources. Previous work describes the SPICE implementation and characterization of these subsystems [1].

Figure 1 also shows a phase lead controller for closed-loop sensor operation. There are many alternatives to this choice of controller, but it should be stressed that closed-loop feedback control offers higher performance as compared to other means for damping the mechanical response of the proof mass [1].

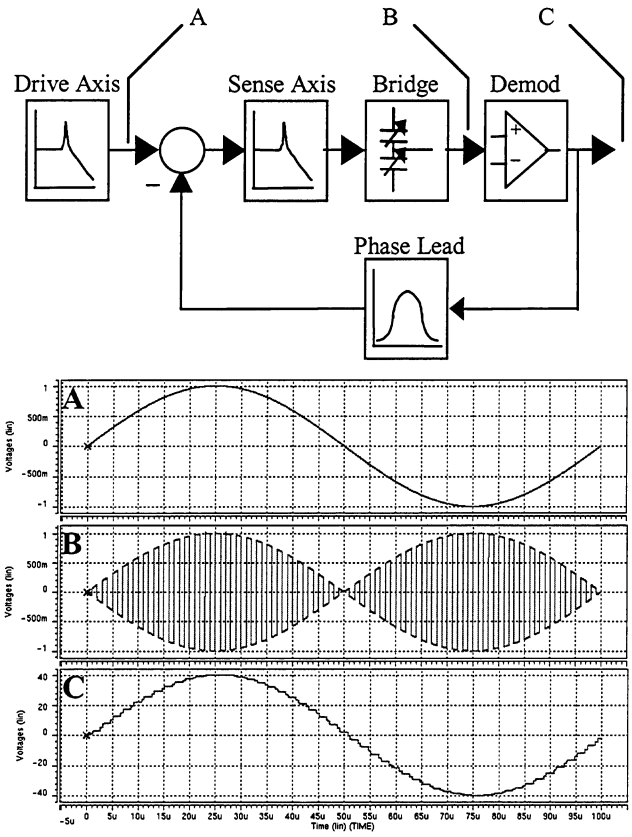

Figure 1 Rate gyro schematic and signals

Figure 1a shows the input rotation (or acceleration) signal, which for inertial sensors will be sinusoidal. The input signal to the measurement circuit is shown in Figure 1b. Information on proof mass position is contained in the low-frequency sine wave envelope created by the multiplication of the high-frequency modulation signals with the input signal. The measurement circuit recovers the amplitude of the AM wave, resulting in the "staircase" sine wave shown in Figure 1c as the sensor output. The shape of the output signal is characteristic of switched-capacitor circuits. The amplitude of the bridge output voltage continues to change during the measurement process, yet once sampled for measurement the stored amplitude voltage cannot be updated until the next cycle of the sampling clock.

Note that the system shown in Figure 1 also applies to an accelerometer model, with the removal of the drive axis. With the exception of quadrature error, a vibratory rate gyro can be considered a Coriolis accelerometer.

2.1 Lock-In Detection

While not a part of the sensor model, a lock-in amplifier model is used as an analytical tool to obtain magnitude and phase information from time-domain simulation. Figure 2 shows a schematic view of a lock-in amplifier. A direct implementation of this model was constructed for use in the SPICE codesign tool.

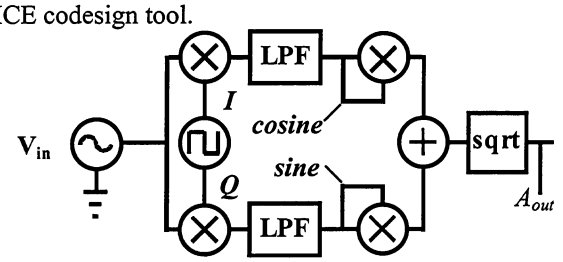

Figure 2 Schematic of lock-in amplifier model

Originally developed as a bandwidth-limiting technique for signal recovery in poor SNR applications, the lock-in amplifier remains a classically simple yet powerful technique for data acquisition [2]. The operation is as follows: We wish to recover the amplitude and phase of a weak periodic signal (V_{in} in Figure 2). V_{in} is multiplied by reference signals I and Q (at the same frequency as V_{in}, but with 0 and 90 degree phase shifts, respectively). The result is low-pass filtered, and the signals that remain are:

$$\text{cosine} = \frac{2A_{in}}{\pi}\cos(\varphi_{in}) \tag{1}$$

$$\text{sine} = \frac{2A_{in}}{\pi}\sin(\varphi_{in}) \tag{2}$$

Magnitude and phase are then calculated as follows:

$$A_{out} = \frac{\pi}{2}\sqrt{(\text{cosine})^2 + (\text{sine})^2} \tag{3}$$

$$\varphi_{out} = \text{atan}\left(\frac{\text{sine}}{\text{cosine}}\right) \tag{4}$$

The lock-in amplifier is used for characterization of individual components and complete sensor systems as well as noise and error signals. The corner frequency of the low-pass filters plays a critical role in determining factors such as distortion and simulation runtime [3][4].

3 NOISE MODELING

The following figure identifies the types and locations of noise sources in the inertial microsensor model.

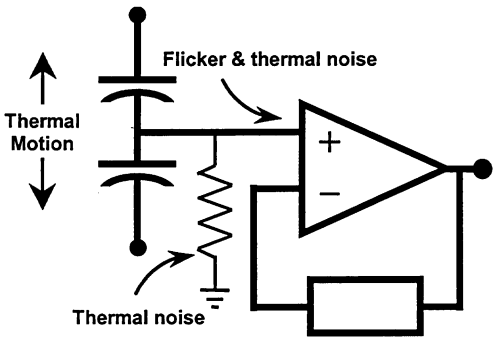

Figure 3 Noise source types and locations

3.1 Thermal Motion of Proof Mass

The thermal noise equivalent acceleration is given by:

$$\ddot{x}_{TNEA} = \sqrt{\frac{4k_b T\omega_0}{mQ}} \quad (5)$$

k_b is Boltzmann's constant, T is the ambient temperature and ω_0 is the resonant frequency of proof mass m with quality factor Q. Thus thermal noise decreases with increasing mass and quality factor. One further observation of interest can be made by noting that

$$\frac{\omega_0}{mQ} = \frac{b}{m^2} \text{ since } Q = \frac{m\omega_0}{b} \quad (6)$$

The parameter b is the damping coefficient. Substituting into the thermal noise acceleration equation:

$$\ddot{x}_{TNEA} = \sqrt{\frac{4k_b Tb}{m^2}} \quad (7)$$

Note thermal noise increases with increased damping, a somewhat counterintuitive result.

3.2 Flicker Noise in MOS Transistors

Flicker noise is another noise mechanism in MOS devices associated with current flow (other than the temperature-dependent "resistance" of the channel), and this noise phenomenon is a direct function of the channel dynamics experienced by carriers as they travel from source to drain. In particular, some carriers passing just beneath the substrate-gate oxide interface in the channel will periodically become trapped in or released from the gate oxide insulating layer.

$$v^2_{flicker} = \frac{K_f}{C_{ox}WL}\frac{1}{f} \quad (8)$$

K_f is a process-dependent parameter that indicates how "clean" the fabrication process is, C_{ox} is the gate oxide per unit area, W and L are the drawn transistor geometry and f is frequency. Note that while flicker noise seems heavily weighted towards "slow" trap-and-release events, current MOS processes exhibit knee frequencies nearing 1MHz.

NMOS transistors exhibit higher values of K_f than PMOS, and this difference is probably due to several confounding factors. First, PMOS devices utilize a "buried" channel that is some distance from the oxide-substrate interface. Secondly, the mobility of holes (PMOS) is less than that of electrons (NMOS), resulting in fewer charge carriers (i.e., current) for a given gate-source overdrive voltage. The likelihood of carrier trapping decreases with fewer carriers traversing the channel.

To incorporate thermal motion into microsensor simulation, an arbitrary (ideally infinite) number of sine wave voltage sources are created with appropriate frequency and amplitude (given by equation 5) and random phase. Modeling flicker noise follows the approach for thermal motion of the proof mass, except the amplitude is defined by the square root of equation 8.

3.3 Noise Frequency Spectra

Flicker and thermal noise components create a dichotomous noise spectra, with flicker noise dominating at low frequencies. Flicker and thermal noise components are equal at the knee frequency, and for frequencies greater than this value thermal noise is the dominant mechanism. As MOS processing steadily progresses to smaller minimum feature sizes (denoted by L_{min} in Figure 4) the knee frequency has steadily increased also.

Figure 4 shows the noise spectrum typically encountered in inertial microsensor design. Note the thermal noise floor is determined by the higher of the thermal motion of the proof mass and the thermal noise of the interface circuit.

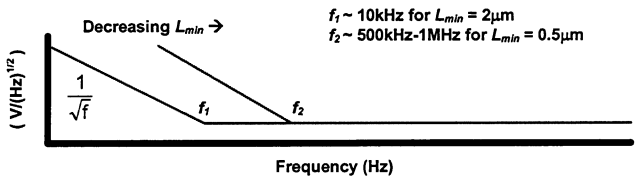

Figure 4 Typical microsensor noise spectrum

4 RESULTS AND DISCUSSION

Flicker noise sources were created using the method just described and run in transient simulation (Figure 6). Flicker noise coefficients were extracted from measured data for a 0.6μm CMOS process as reported in [5]. Amplitudes were scaled according to transistor width [4]. The following figure compares the PSD for each source, showing scalability with transistor size. The ratio of powers is 5.3, an error of approximately 6%.

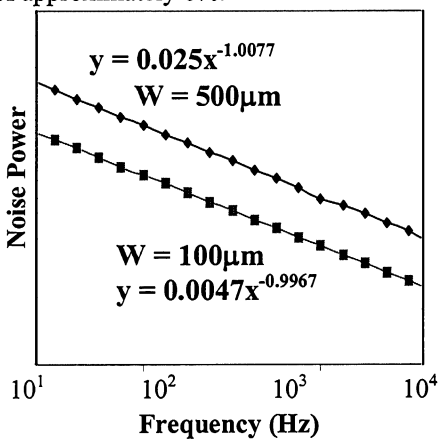

Figure 5 Flicker noise power spectral density

The frequency at which the measurement circuit operates should be higher than the knee frequency to avoid upconverting flicker noise to the modulation frequency,

thereby further corrupting the acceleration amplitude measurement.

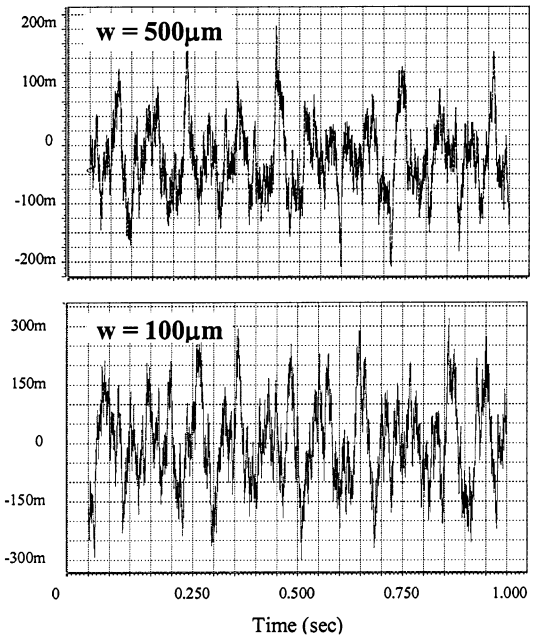

Figure 6 Transient flicker noise waveforms

For 2μm generation designs, flicker noise was only a concern for very low frequency signal processing. As the knee frequency approaches 1MHz in current processes, however, microsensor interface circuits must operate at frequencies in excess of 10MHz, placing additional design tradeoffs with settling time, power dissipation and linearity. The selection of mechanical resonance frequency is also affected by the knee frequency, as sensor sensitivity incorporates responsivity (mechanical resonance) and noise (flicker and thermal). The various tradeoffs involved in noise, signal level and frequency of operation are completely addressed in [4], as is the impact of increasing knee frequency on inertial microsensor performance.

The comb of sine sources and lock-in amplifier model can also be used to obtain frequency response data from transient simulation.

Figure 7 shows magnitude (top) and phase (bottom) comparison between the lock-in amplifier and an FFT for a three-stage CMOS ring oscillator (with resonance at 102.2MHz). Note the lock-in amplifier is able to follow the phase of the nonlinear system with better fidelity than the more conventional transform, while also providing accurate magnitude information. Phase determination is critical in rate gyro design for management of quadrature error [1][4].

As implemented in SPICE the FFT is inadequate for determination of frequency spectra for high performance inertial microsensors. Such sensors require low resonant frequency for maximum responsivity. Furthermore, high Q suspensions are needed to minimize thermal motion (see equation 5). The FFT algorithm in SPICE is limited to 1Hz resolution, and thus cannot faithfully reproduce the sharp resonance peak at low frequencies [3].

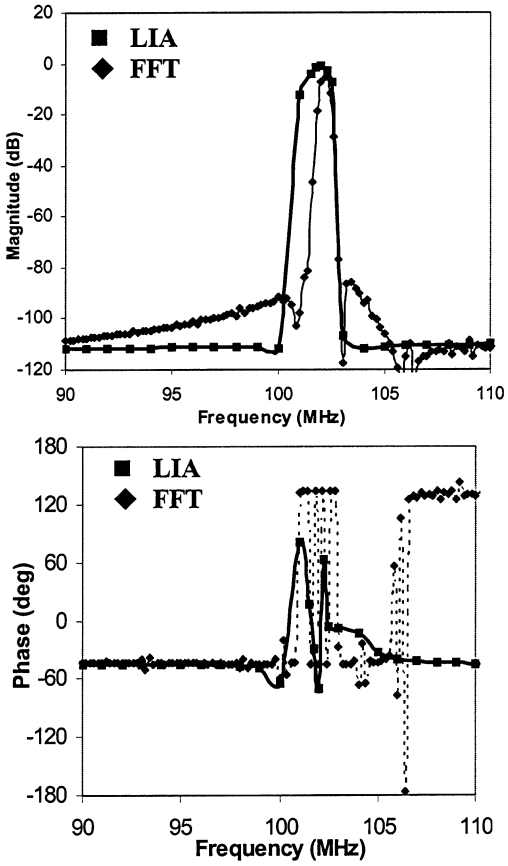

Figure 7 VCO transfer function

5 ACKNOWLEDGMENTS

This research was supported by the DARPA/TRP program and the Jet Propulsion Laboratory.

REFERENCES

[1] M.D. Pottenger and W.J. Kaiser, "First Discrete Time Full-System Inertial Microsensor Performance Simulation Tool", *Proc. Intl. Mech. Eng. Congress and Exhibition*, vol. DSC-66, pp. 519-524, 1998.

[2] M.L. Meade, "*Lock-In Amplifiers: Principles and Applications*", Peter Peregrinus for IEE, 1989.

[3] M.D. Pottenger and W.J. Kaiser, "MEMS Codesign: First Full-System Inertial Microsensor Design Tool", *Proc. Intl. Mech. Eng. Congress and Exhibition*, vol. DSC-66, pp. 583-588, 1998.

[4] M.D. Pottenger, "Design of Micromachined Inertial Sensors", Ph.D. dissertation, Univ. of Cal. at Los Angeles, Dept. of Elec. Eng., 2000.

[5] B.R. Schiffer, A. Burstein and W.J. Kaiser, "An Active Charge Cancellation System for Switched-Capacitor Sensor Interface Circuits", *IEEE J. of Solid State Circuits*, vol. 33, no. 12, pp. 2134-2138, 1998.